ROYAL SOCIETY
OF CHEMISTRY

PAPER

Check for updates

Enhanced physical, mechanical and barrier properties of chitosan films *via* tannic acid cross-linking

Supachok Tanpichai, [ID] *[ab] Kitti Yuwawech,[cd] Ekachai Wimolmala,[ce] Yanee Srimarut, [ID] [f] Weerapong Woraprayote [ID] [fg] and Yuwares Malila [ID] [f]

Growing environmental concerns over the extensive use of petroleum-based polymer packaging have spurred interest in the development of bio-based alternatives. In this work, the incorporation of tannic acid as a cross-linker into chitosan at concentrations of 0–60 wt% was explored. The resulting cross-linking between chitosan chains induced by tannic acid through hydrogen and Schiff-base covalent bonding was confirmed by X-ray photoelectron spectroscopy and gel content measurements. This significantly enhanced the films' thermal stability, water uptake, mechanical properties, and barrier properties. The cross-linking minimized the interaction between chitosan functional groups and water molecules, improving water resistance. The chitosan films with 30 wt% tannic acid displayed significant improvements in tensile stress and Young's modulus by 74% and 110%, respectively, compared with the neat chitosan films, which were ascribed to the strong interaction between chitosan and tannic acid. In addition, the cross-linked films effectively blocked UV light transmission while maintaining transparency levels greater than 85%, offering potential protection against photo-oxidation and photo-discoloration of food produce caused by sunlight exposure. However, increasing tannic acid loading negatively affected the antibacterial properties, wettability, and appearance (increased yellowness) of the cross-linked chitosan films. Furthermore, packaging developed from these cross-linked chitosan films successfully extended the shelf life of chilies, demonstrating their application in food packaging. Compared with petroleum-based polymers and biopolymer packaging films, these cross-linked chitosan films offer promising mechanical and barrier properties and UV-shielding capability, making them a sustainable alternative for packaging applications.

[a]Learning Institute, King Mongkut's University of Technology Thonburi (KMUTT), Bangkok, 10140, Thailand. E-mail: supachok.tan@kmutt.ac.th

[b]Cellulose and Bio-based Nanomaterials Research Group, King Mongkut's University of Technology Thonburi (KMUTT), Bangkok, 10140, Thailand

[c]Division of Materials Technology, School of Energy, Environment and Materials, King Mongkut's University of Technology Thonburi (KMUTT), Bangkok, 10140, Thailand

[d]Office of the Permanent Secretary, Ministry of Higher Education, Science, Research and Innovation (MHESI), Bangkok, 10400, Thailand

[e]Polymer PROcessing and Flow (P-PROF) Research Group, School of Energy, Environment and Materials, King Mongkut's University of Technology Thonburi (KMUTT), Bangkok, 10140, Thailand

[f]National Center for Genetic Engineering and Biotechnology (BIOTEC), Pathum Thani, 12120, Thailand

[g]Department of Biochemistry, Siriraj Metabolomics and Phenomics Center (SiMPC), Faculty of Medicine Siriraj Hospital, Mahidol University, Bangkok, 10700, Thailand

1 Introduction

To live without plastics might be impossible for humans. Their mass production has begun since the 1950s.[1,2] After World War II, plastic consumption skyrocketed, leading to an exponential increase in plastic waste within municipal solid waste streams.[1–3] According to the information of 2005, approximately 6300 million tons of plastic waste was estimated to be generated, with only 9% being recycled, 12% incinerated, and around 79% accumulated in landfills and oceans.[1,3,4] The main application of plastics is packaging, with a paradigm shift from reusable to single-use purposes due to the emergence of the COVID-19 pandemic,[5] leading to a significant increase in waste accumulation. Today, one substantial concern of plastics is that they can undergo fragmentation into smaller particles, called microplastics and nanoplastics, through processes such as photodegradation, mechanical abrasion, and oxidation. Microplastics and nanoplastics have been extensively found in the environment and living creatures, including in wildlife, aquatic animals, and even humans.[2] These significant concerns have led to the development of biodegradable and environmentally friendly packaging materials from biodegradable polymers as alternatives to traditional petroleum-based plastics.[3,6–8]

With an estimated 464 billion USD market share in global food packaging by 2027, the development of biodegradable and environmentally friendly packaging has been of global interest.

Biopolymers derived from polysaccharides, cellulose, and proteins for packaging applications have gained considerable attention due to their promising advantages of nontoxicity, sustainability, biocompatibility, and biodegradability.[3,4,6,7,9–11] Among these biopolymers, chitosan, a polysaccharide derived from chitin extracted from the exoskeletons of crustaceans such as crab or shrimp and mushrooms through deacetylation, exhibits abundance, antimicrobial properties, solubility in acidic solvents, film-forming ability, and promising mechanical properties.[12–15] Chitosan has found extensive applications in extending the shelf life of fresh food produce and meat and has also been fabricated into biodegradable packaging films.[13–16] However, the presence of chitosan's numerous amino and hydroxyl groups and hydroxyl or aldehyde groups at its chain ends makes it hydrophilic and sensitive to water, potentially limiting its applications especially when exposed to aqueous environments.[17,18] Therefore, the development of biodegradable chitosan films with reduced hydrophilicity and water absorption can be a promising approach to significantly broaden their range of applications.

Tannic acid, a polyphenol compound derived from plants such as wood and tea leaves, provides several advantages such as water solubility, reasonable cost, antibacterial properties, and the presence of multiple phenolic hydroxyl groups that can interact with other macromolecules. Thus, tannic acid has been employed as a natural cross-linker with biopolymers such as gelatin, cellulose, and poly(vinyl alcohol).[3,19–24] Tannic acid is generally recognized as safe by the US Food and Drug Administration.[23] Chen et al.[25] reported that tannic acid formed cross-links with poly(vinyl alcohol), thereby improving the mechanical properties of the hydrogels. Similarly, the strong interaction between tannic acid and poly(vinyl alcohol) considerably reduced the water uptake of the aerogels and significantly improved their mechanical performance.[21] Moreover, Kaczmarek et al.[26] incorporated tannic acid into chitosan to prepare chitosan films with enhanced mechanical properties and surface free energy. With the increase in tannic acid loading up to 50 wt%, an increase in surface free energy and tensile stress of the films was observed. However, this work focused on investigating the surface free energy and mechanical properties of the chitosan films at tannic acid loadings of 0–50 wt%. Another study by Lee et al.[27] reported improved properties and antibacterial activity of chitosan with tannic acid in two different ratios (chitosan to tannic ratio of 2 : 1 and 2 : 2).

Although several studies have explored the potential of tannic acid as a cross-linker for chitosan, its application in developing sustainable chitosan-based packaging films remains underexplored.[26–29] Therefore, this work provides insights into the use of tannic acid for improving the properties and water resistance of chitosan films for packaging applications. Herein, we developed the chitosan films incorporating tannic acid and evaluated the influence of tannic acid concentrations of 0–60 wt% on the physical, mechanical, and barrier properties of the chitosan films. Moreover, we assessed the water sensitivity, UV-shielding capability, and antibacterial properties of the chitosan films with different tannic acid concentrations. Furthermore, preliminary investigation on the packaging developed from these chitosan films with tannic acid was conducted to evaluate its effect on the shelf life of chilies. Given the limited exploration of the use of tannic acid with chitosan for developing cross-linked chitosan-based films, this study offers a straightforward approach with a suitable tannic acid loading for the fabrication of biodegradable films with improved mechanical and barrier properties and reduced water sensitivity for food packaging applications.

2 Experimental

2.1 Materials and chemicals

Commercial-grade chitosan powder with a molecular weight of 2100 kDa and a degree of deacetylation of 92.25% (SSA190/3k8k) was purchased from Marine Bio Resources Co., Ltd (Thailand). Tannic acid (Cat. No: 419995000, ACS grade) as a cross-linker was procured from Thermo Fisher Scientific (USA), and glacial acetic acid (≥99.85%) was obtained from Sigma-Aldrich (USA).

2.2 Preparation of cross-linked chitosan films with tannic acid

Chitosan was continuously stirred in a 1 wt% acetic acid solution at room temperature (25 ± 3 °C) for 24 h to obtain a clear solution with a concentration of 0.75 wt%. Various concentrations of tannic acid (0–60 wt%) were gently added to the chitosan solutions, and these mixtures were stirred overnight. Afterward, the solutions were poured into Petri dishes and oven-dried at 40 °C. Finally, the cross-linked chitosan films were successfully obtained, which are denoted as "TX," where "X" is the weight fraction of tannic acid in the films.

2.3 Optical properties and UV-shielding capability

The light transmittances of the chitosan films with tannic acid were determined using a UV-vis spectrophotometer (UV-3100, Shimadzu Corp., Japan) in the wavelength range of 250–1000 nm, following the ISO 9050 standard method. Moreover, the color properties of the chitosan films with different tannic acid concentrations were measured using a UV-3100 spectrophotometer (Shimadzu Corp., Japan). The whiteness index (WI) and yellowness index (YI) were determined based on ASTM E313-20.[11] UV-blocking efficiencies (%) were calculated from the average transmittance of UV-A (315–400 nm) and UV-B (280–315 nm) using the following equations:[30–32]

$$\text{UV-A blocking } (\%) = 100 - \left(\frac{\sum\limits_{315}^{400} T(\lambda)d(\lambda)}{\sum\limits_{315}^{400} d(\lambda)} \right) \quad (1)$$

$$\text{UV-B blocking } (\%) = 100 - \left(\frac{\sum\limits_{280}^{315} T(\lambda)d(\lambda)}{\sum\limits_{280}^{315} d(\lambda)} \right) \quad (2)$$

where $T(\lambda)$ is the average transmittance of the chitosan films at the wavelength of λ, and $d(\lambda)$ is the bandwidth of the film.

Furthermore, the cross-linked chitosan film with 30 wt% tannic acid (T30) was placed and secured on a vessel, and two thermocouples were positioned above and beneath the film to monitor the temperature. The film-mounted vessel was subsequently exposed to a UV LED light at 395 nm and artificial sunlight generated by a solar simulator (ORIEL LS-100, Newport Corp., USA) coupled with a 1 kW xenon arc lamp for 60 min. Temperatures above and below the film were recorded using a thermal scanner (Seek Thermal, Inc., USA). This process was modified from a previous study.[33] As control, a 1 mm-thick glass substrate was placed on a vessel, and the temperature difference was evaluated using the aforementioned procedure.

2.4 Chemical structure

The chemical structures of the chitosan films with different tannic acid concentrations were analyzed using a Nicolet iS5 Fourier-transform infrared (FTIR) spectrometer (Thermo Scientific, USA), equipped with iD5 attenuated total reflectance accessory, over the wavenumber range of 600–4000 cm^{-1} at a resolution of 4 cm^{-1} with a total of 32 scans. Moreover, X-ray photoelectron spectroscopy (XPS) analysis was performed using an AXIS Supra (Shimadzu Corp., Japan) equipped with a monochromatic Al Kα X-ray source operating at 15 mA to investigate the interactions between chitosan molecules and tannic acid.

2.5 Crystallinity

To characterize the crystal structures, the prepared films were studied by X-ray diffraction (XRD) (D8 Discover XRD, Bruker AXS, Germany), equipped with a Goebel mirror with CuKα radiation (wavelength of 0.1540 nm) at an accelerating voltage of 40 kV and a current of 40 mA. The samples were scanned in the 2θ range of 5°–60° with a step size of 0.02° and step speed of 0.8 s.

2.6 Thermal stability

The thermal stabilities of the cross-linked chitosan films with different tannic acid concentrations were characterized by thermogravimetric (TG) analysis (TG-209F3, NETZSCH-Gerätebau GmbH, Germany). Approximately 10 mg of each sample was initially heated to 110 °C and held for 20 min to remove moisture. Then, the sample was scanned to 800 °C at a heating rate of 10 °C min^{-1} under a nitrogen atmosphere.

2.7 Gel content and water uptake

The preweighted oven-dried cross-linked chitosan samples (W_0) were immersed in 25 mL of 5 wt% acetic acid for 24 h. Afterward, the remaining parts of the samples were collected, oven-dried at 60 °C for 24 h, and weighted (W_f). The gel contents of the cross-linked chitosan films were determined using the following formula:[34,35]

$$\% \text{ Gel content} = \left(\frac{W_f}{W_0}\right) \times 100 \qquad (3)$$

Meanwhile, the water uptakes of the chitosan films with different tannic acid loadings were examined. The oven-dried samples (10 mm × 10 mm) were initially weighted (W_i) and immersed in distilled water at a temperature of 25 ± 3 °C. The samples were removed and weighed (W_t) at specific interval times of 1, 2, 4, 6, 8, 24, 48, and 72 h. Before weighing the samples, any remaining water on the film surfaces was carefully removed by tissue. The measurements were performed in triplicate, and the water uptakes of the chitosan films with different tannic acid concentrations were calculated using the following equation:[35]

$$\% \text{ Water uptake} = \left(\frac{W_t - W_i}{W_i}\right) \times 100 \qquad (4)$$

2.8 Wettability

The wettabilities of the chitosan films cross-linked with tannic acid were evaluated using a SL150E contact angle meter (KINO Scientific Instrument Inc. (USA)) equipped with a high-resolution CCD camera. A droplet of distilled water was dropped on the surface of a film sample, and the contact angle between the water droplet and the film surface was measured at the point of contact.

2.9 Mechanical properties

The tensile properties of the cross-linked chitosan films with tannic acid were determined using a universal testing machine (5583, Instron Corp., USA) equipped with a 5 kN load cell. Rectangular samples with a width of 5 mm and length of 50 mm were placed between two grips with a gauge length of 20 mm and tested at a crosshead speed of 5 mm min^{-1}. Averages and standard deviations of the tensile strength, Young's modulus, and tensile strain were calculated from at least five samples for each material.

2.10 Barrier properties

The water vapor transmission rate (WVTR) and oxygen transmission rate (OTR) of the cross-linked chitosan films with different tannic acid concentrations were calculated. WVTRs were determined based on the modified ASTM E96-95. A dried sample with a size of 50 mm × 50 mm (W_a) was placed inside a household WVTR tool kit filled with 25 g of silica gel and stored at a relative humidity of 75% for 1 day (t). Afterward, the samples were weighted (W_w). Measurements were performed in triplicate. The WVTRs of the cross-linked chitosan films were calculated using the following equation:

$$\text{WVTR} = \left[\frac{(W_w - W_a) \times T}{t \times A}\right] \qquad (5)$$

where T and A are the thickness (mm) and exposed area (m^2) of the film, respectively, and the unit of WVTR values is g mm per m^2 per day.

The OTRs of the circular-shaped cross-linked chitosan films with a diameter of 5 cm were determined using an OX-TRAN 1/50 analyzer (Ametek Mocon, Inc., USA) at a temperature of 25 ± 3 °C and a relative humidity of 0%. The film sample was placed

between two semi-chambers with continuous flushing of nitrogen gas. Then, oxygen gas was purged from the bottom chamber, and oxygen molecules permeated through the film to the upper chamber. The OTR was expressed in cm^3 per m^2 per day.

2.11 Morphology

The fracture surfaces of the cross-linked chitosan films with different tannic acid loadings after tensile deformation were examined using a FEI Nova NanoSEM field-emission scanning electron microscope (USA). Before imaging, all samples were coated with a thin layer of gold to improve conductivity.

2.12 Antibacterial properties

The antimicrobial properties of the cross-linked chitosan films were evaluated using an agar diffusion assay against *Escherichia coli* ATCC 25922 (*E. coli*) and *Staphylococcus aureus* ATCC 25923 (*S. aureus*). Briefly, the circular-shaped cross-linked chitosan films with a diameter of 5 mm were prepared and positioned on a sterile plate containing pre-set tryptic soy broth mixed with 1.5% agar (*i.e.*, TSA layer). Subsequently, a 7 mL molten tryptic soy broth mixed with 1% agar (TSA soft agar layer), containing approximately 6 log CFU mL^{-1} of the tested bacterium, was overlaid onto the top of the film samples. All plates were then incubated at 37 °C for 24 h. The ability of the films to inhibit the tested bacteria was determined by the presence of a clear zone in contact with and around the film samples.

2.13 Application of the films for packaging

The cross-linked chitosan films with the optimum properties were selected to develop the packaging. Chilies (*Capsicum annuum*), kindly provided by a local farmer in Thailand, were placed in the prepared chitosan packaging and stored under ambient conditions with a temperature of 25 ± 3 °C and relative humidity of 50 ± 10% for 7 days. As control, chilies were stored without the use of any packaging. The appearances of these chilies were photographed to assess their shelf life.

2.14 Statistical analysis

Statistical analysis was performed using SPSS Statistics 29.0. To determine significant differences between datasets ($p < 0.05$), one-way analysis of variance (ANOVA) was employed. *Post hoc* analysis to identify significant differences in the means was subsequently performed using Duncan's multiple range test.

3 Results and discussion

3.1 Transmittance and UV-shielding performance

Fig. 1(a and b) presents the appearance and UV-vis spectra of the chitosan films with different tannic acid loadings in 250–1000 nm. The chitosan films without tannic acid (T0) were clear and colorless, with WI of 96.1 ± 0.1 and YI of 1.5 ± 0.1. However, introducing tannic acid changed the appearance of T10 from clear to yellowish, with WI of 93.1 ± 0.4 and YI of 6.3 ± 0.6. With the increase in tannic acid concentration, the color of

yellowish and brownish became more pronounced. For example, T20 had WI of 88.8 ± 1.0 and YI of 13.6 ± 1.5. This shift in color of the chitosan films was caused by the yellowish hue of tannic acid. Greater than 20 wt% tannic acid, there were no significant change observed in the WI and YI. Moreover, Table 1 shows the transmittance of the chitosan films with various tannic acid loadings. The T0 film exhibited high transparency, with a transmittance of 91.2 ± 0.1% at 600 nm. However, the transmittance at 600 nm of the chitosan films slightly decreased to 88.0 ± 0.3% and 86.3 ± 0.7% with 10 and 20 wt% tannic acid, respectively. Notably, with tannic acid concentrations exceeding 20 wt%, no further changes in a 600 nm light transmittance were observed. The reduction in transmittance may be owing to the cross-linking formed within the films.

Considering that UV radiation can lead to photo-oxidation, affecting food quality and sensory characteristics,[32,36] the UV-blocking efficiencies of the chitosan films with tannic acid were evaluated (Fig. 1(c)). When tannic acid was introduced, the chitosan films showed superior UV-blocking capability for both UV-B (280–315 nm) and UV-A (315–400 nm).[37,38] The T0 films demonstrated UV-B and UV-A blocking efficiencies of 20.4% and 33.4%, respectively. A notable enhancement in UV-blocking efficiencies was observed with incorporating tannic acid. The T10 films exhibited UV-B and UV-A blocking efficiencies of 99.8% and 77.3%, respectively. An increase in tannic acid concentration resulted in chitosan films effectively blocking all UV-B rays (no UV-B rays transmitted through the films) and demonstrated a significant improvement in UV-A blocking efficiency. Specifically, the T30 films exhibited a UV-A blocking efficiency of 89.8%. However, at greater than 30 wt% tannic acid, no significant change in UV-A and UV-B blocking efficiencies was observed. The UV-blocking capability of these chitosan films with tannic acid was attributed to the absorbance of UV light by polyphenolic compounds and ketones of tannic acid, which are UV-absorbing chromophores.[39,40] The UV-A and UV-B blocking efficiencies of the chitosan films incorporating tannic acid were found to be superior to those of petroleum-based and biodegradable packaging films.[41,42]

Moreover, with more than 30 wt% tannic acid, these chitosan films demonstrated similar UV-blocking efficiencies and transparencies. Therefore, the T30 films were selected to further study their UV-shielding capability. The T30 film-mounted vessel was exposed to a UV LED light and 1 kW xenon arc lamp-generated artificial sunlight, and the temperature above and below the film was recorded for 60 min to obtain a graph of the temperature difference as a function of exposure time, as shown in Fig. 1(d). When sunlight hits a surface, heat conduction and radiation occur.[33] Upon exposure to both UV LED light and artificial sunlight, the temperature inside the vessels continuously increased. The temperature differences of the T30 film after 60 min exposure time (~2.5 °C under a UV LED light and ~6.9 °C under sunlight) were considerably higher than the 1 mm-thick glass substrate (~2.1 °C under a UV LED light and ~5.8 °C under sunlight), which was attributed to reduced UV radiation transmission compared with the glass substrate. It would be noteworthy that the T30 films had a thickness of ~30
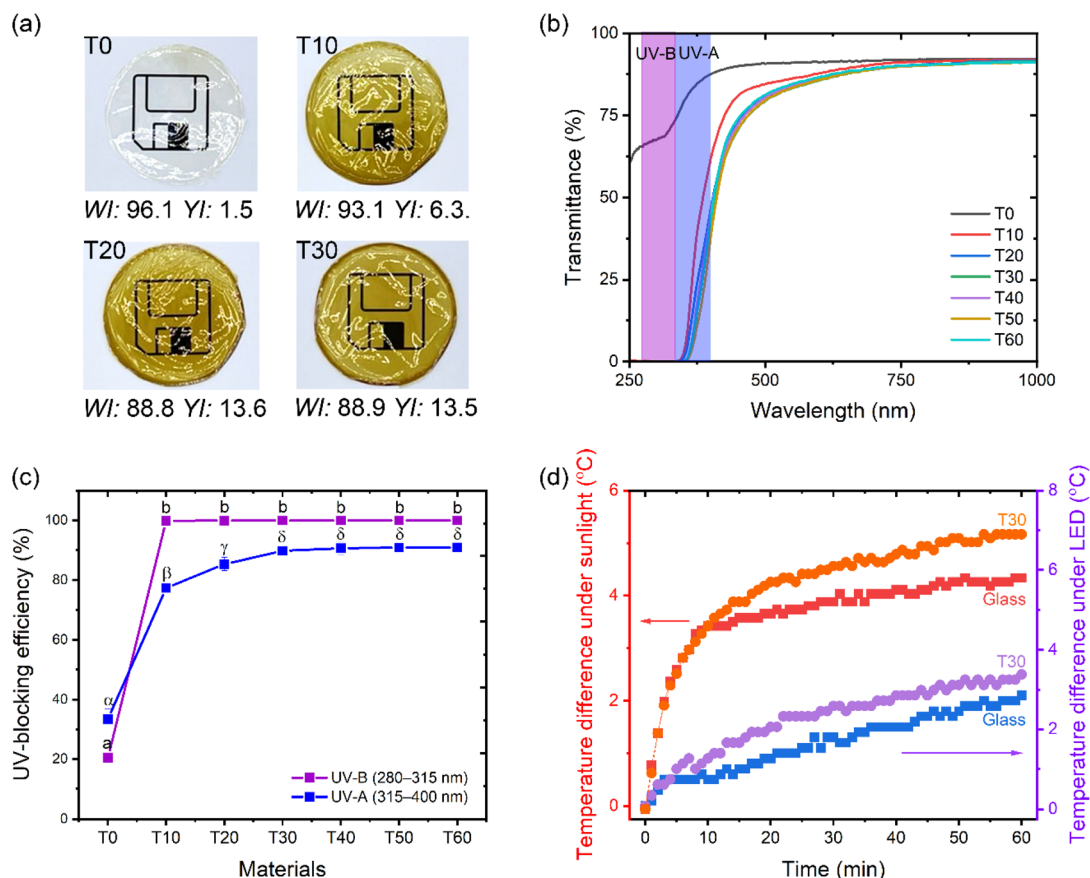
Fig. 1 Optical properties of the chitosan films with different tannic acid concentrations: (a) film appearance, (b) UV-vis spectra, and (c) UV-blocking efficiencies. (d) Temperature difference between the upper and lower sections of the chitosan film with 30 wt% tannic acid (T30) and the 1 mm-thick glass substrate used as control, plotted against exposure time under UV LED light (395 nm) and artificial sunlight generated by a solar simulator coupled with a 1 kW xenon arc lamp for 60 min. Superscript letters in the figure represent significant differences ($p < 0.05$) among the samples tested under the same conditions.

Table 1 Transmittance of the chitosan films with tannic acid at 280–315, 315–400, and 600 nm. Superscript letters represent significant differences ($p < 0.05$) among the samples tested under the same conditions

Materials	Light transmittance (%)		
	280–315 nm	315–400 nm	600 nm
T0	79.570 ± 1.509^a	66.6 ± 3.4^a	91.2 ± 0.1^a
T10	0.160 ± 0.014^b	22.7 ± 1.4^b	88.0 ± 0.3^b
T20	0.079 ± 0.004^b	14.7 ± 2.2^c	86.3 ± 0.7^c
T30	0.052 ± 0.005^b	10.2 ± 1.1^d	85.6 ± 0.3^c
T40	0.034 ± 0.003^b	9.3 ± 2.2^d	85.4 ± 0.9^c
T50	0.030 ± 0.002^b	9.1 ± 0.8^d	86.1 ± 0.3^c
T60	0.023 ± 0.002^b	9.1 ± 1.5^d	86.3 ± 0.5^c

μm. Therefore, increasing the film thickness would significantly enhance its UV-shielding performance. These chitosan films with tannic acid, exhibiting excellent UV-shielding capability alongside high transparency (more than 85%), hold promise for food packaging, offering protection of food items against photo-oxidation and photo-discoloration caused by sunlight radiation. Thus, these films can extend the shelf life of food products.

3.2 Chemical structure and crystallinity

The chemical structures of the chitosan films with tannic acid were evaluated and are illustrated in Fig. 2(a and b). The chitosan films displayed several typical characteristic bands such as 1630 cm^{-1} (C=O stretching of amide I), 1553 cm^{-1} (N–H bending vibration of amide II), 1413 cm^{-1} (stretching vibration of amino groups), and 1250 cm^{-1} (N–H co-bending vibration of amide III).[7,43] The bands at 1040–1150 cm^{-1} are attributed to the C–O–C stretching in the glycosidic bonds of chitosan.[7,43,44] The broad absorption band located at 3000–3600 cm^{-1} (O–H and N–H stretching vibration) and duplet bands located at 2880 cm^{-1} (asymmetric and symmetric C–H stretching vibration) were also observed for the chitosan material.[7,17,45,46]

With introduction of tannic acid, the typical characteristic bands assigned to amide (1553, 1413, and 1250 cm^{-1}) weakened and the broad band intensity at 3000–3600 cm^{-1}, associated with the functional groups of chitosan, diminished. This was ascribed to the interaction between the amino (NH$_2$) and hydroxyl groups of chitosan and phenoxy groups of tannic acid,
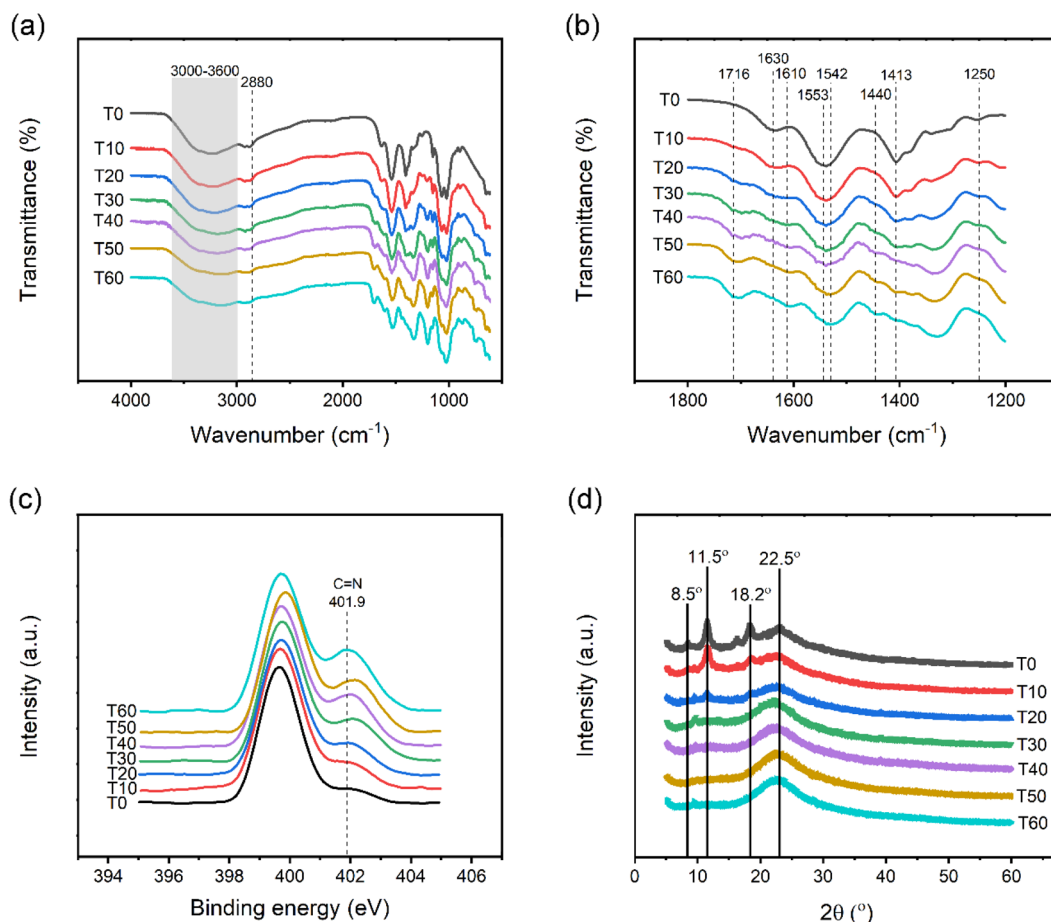
Fig. 2 Chemical characteristics and crystallinities of the chitosan films with different tannic acid concentrations: Fourier-transform infrared (FTIR) spectra in the range of (a) 600–4000 cm^{-1} and (b) 1200–1800 cm^{-1}, (c) N 1s spectra obtained from X-ray photoelectron spectroscopy (XPS), and (d) X-ray diffraction (XRD) patterns.
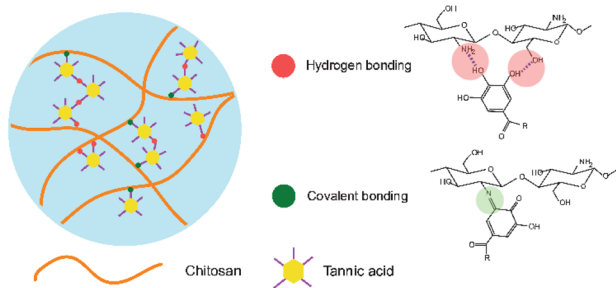

Fig. 3 Illustration of the interactions between chitosan and tannic acid through hydrogen bonding and covalent bonding.

resulting in cross-linking,[27,43] as shown in Fig. 3. Increasing tannic acid loading led to the further weakening of the 1413 and 1250 cm^{-1} bands, corresponding to amide groups. Moreover, the peak at 1553 cm^{-1} shifted to a lower wavenumber with higher tannic acid concentrations, possibly due to the protonation of the amino group by excess tannic acid, leading to the formation of ammonium groups (NH$_3^+$) within the chitosan structure. Moreover, during film preparation, chitosan was dissolved in an acetic acid solution, where protons released from the acid could interact with amino groups of chitosan, resulting in their protonation to form NH$_3^+$.[47,48] An additional peak located at 1440 cm^{-1} related to the interactions between the NH$_3^+$ and phenolic hydroxyl groups of tannic acid through hydrogen bonding was observed for the cross-linked chitosan films with less than 30 wt% tannic acid, suggesting that dominant cross-linking occurred via hydrogen bonding between chitosan and tannic acid, which aligns with previous studies.[27,29] The presence of the covalent cross-linking between the amino groups of chitosan and gallol groups of tannic acid was reported at tannic acid concentrations of as low as 1–2 wt%; however, with the increase in tannic acid concentration, the hydrogen bonding interactions between the two components was favored.[27,29] Furthermore, the characteristic bands of tannic acid at 1716, 1610, and 1542 cm^{-1}, corresponding to its aromatic structure, became more pronounced with increased tannic acid content within the films.[43]

To further investigate the interactions between chitosan and tannic acid, XPS analysis was conducted. Fig. 2(c) shows the N1s XPS spectra of the cross-linked chitosan films with various tannic acid loadings. The neat chitosan films (T0) exhibits the binding energies at 398.7 eV, 399.7 eV, and 401.2 eV,
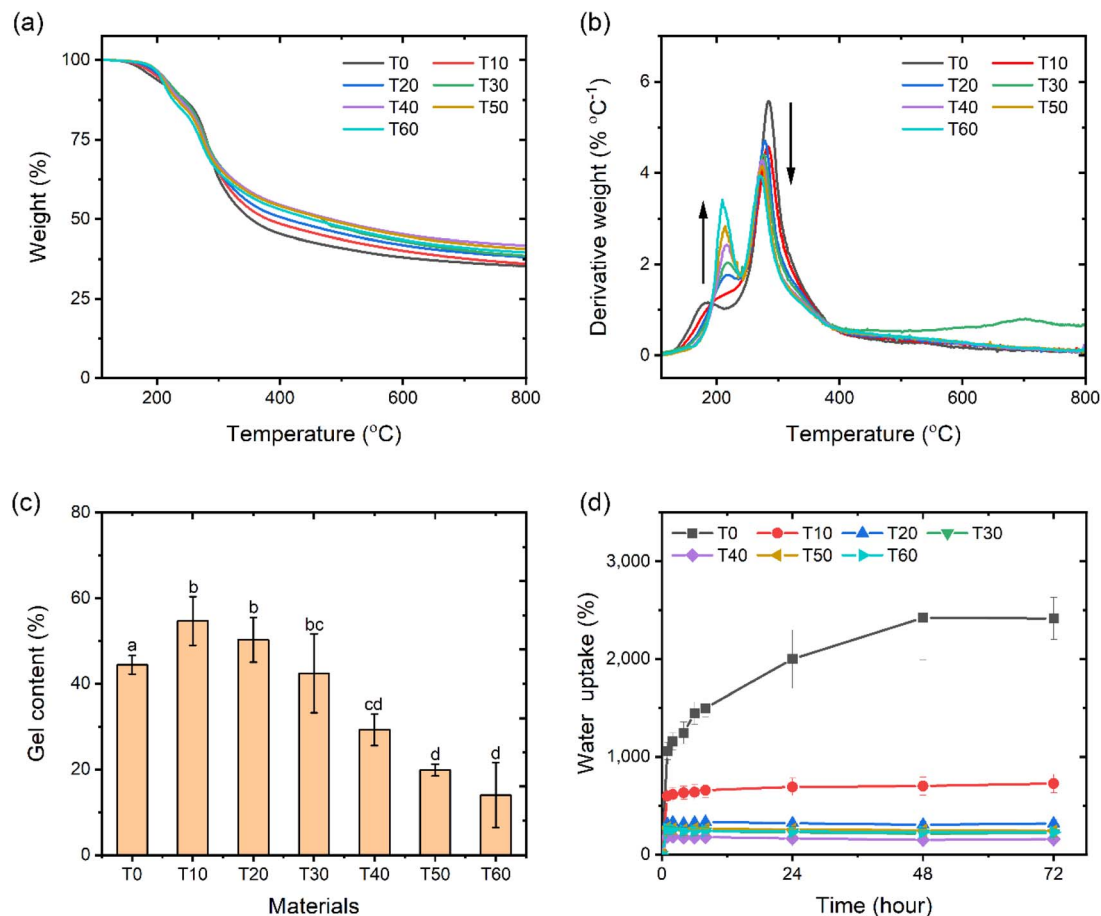
Fig. 4 Thermal stabilities of the cross-linked chitosan films with tannic acid: (a) thermogravimetric (TG) and (b) derivative TG (DTG) curves; (c) gel contents and (d) water uptakes of the chitosan films with different tannic acid loadings. Superscript letters represent significant differences ($p < 0.05$) among the samples tested under the same conditions.

corresponding to NH_2, NH and NH_3^+, respectively.[48] The XPS spectra of the cross-linked chitosan films changed upon incorporation of tannic acid. However, A new peak at 401.9 eV, corresponding to $-C=N-$, was observed. This observation suggests the formation of covalent between the amino groups of chitosan and tannic acid *via* a Schiff base reaction.[27,49] Upon exposure to air, the phenolic hydroxyl groups of tannic acid can be oxidized to form quinone structures.[50–52] These quinone groups contain reactive carbonyl functionalities ($C=O$), which can interact with the primary amino groups of chitosan. This reaction leads to the formation of imine linkages ($-C=N-$), commonly referred to as a Schiff base.[53,54] The intensity of the peak, associated with the imine linkages, became stronger with higher tannic acid concentrations, indicating a greater degree of the covalent cross-linking within the films. Although the intensity of this peak increased with higher tannic acid concentrations, it remained considerably lower than the peaks corresponding to NH_2, NH and NH_3^+. This suggests that both hydrogen bonding and covalent cross-linking were dominant interactions in the chitosan-tannic acid films, as shown in Fig. 3.

Fig. 2(d) presents the XRD patterns of chitosan films with different tannic acid loadings. Chitosan, a semicrystalline polymer, exhibited four typical diffraction peaks at 2θ of 8.5°, 11.5°, and 18.2° and a broad peak at 22.5°.[55–57] The high crystallinity of chitosan was attributed to the intense inter- and intramolecular bonding.[43,58] Addition of tannic acid resulted in a reduction in intensity of the three characteristic peaks at 8.5°, 11.5°, and 18.2°, indicating a shift in the chitosan structure from crystalline to amorphous. This alternation was ascribed to the formation of cross-linking between tannic acid and chitosan molecules.[40,43] Thus, the crystallinity of chitosan decreased. A similar disappearance of these crystalline peaks was observed with incorporation of citric acid.[58] Furthermore, with the increase in tannic acid concentration, the single broad peak located at ~22.5° became more prominent, indicating a larger proportion of the amorphous region. This might be attributed to the increased presence of tannic acid.[25]

3.3 Thermal stabilities

The thermal stabilities of the cross-linked chitosan films with respect to tannic acid concentrations were investigated, and their TG and derivative TG (DTG) curves are presented in Fig. 4(a and b). In addition, Table 2 lists the key thermal degradation parameters of degradation temperature at 1%

Table 2 Degradation temperature at 1% weight loss ($T_{1\%}$), maximum degradation temperatures of the first (T_{max1}) and second (T_{max2}) decomposition stages, char residue content at 800 °C, and water uptake at 72 h immersion time of the cross-linked chitosan films with different tannic acid loadings. Superscript letters represent significant differences ($p < 0.05$) among the samples tested under the same conditions

Materials	$T_{1\%}$ (°C)	T_{max1} (°C)	T_{max2} (°C)	Char content at 800 °C (%)	Water uptake at 72 h immersion time (%)
T0	157.1 ± 1.7[a]	187.6 ± 3.5[a]	285.1 ± 0.4[a]	34.8 ± 1.3[a]	2415.5 ± 215.4[a]
T10	162.5 ± 0.6[b]	202.2 ± 1.3[b]	282.6 ± 0.8[b]	36.7 ± 1.1[b]	725.4 ± 95.2[b]
T20	169.8 ± 1.1[c]	217.4 ± 1.5[c]	278.0 ± 0.2[c]	38.7 ± 0.5[c]	315.7 ± 34.8[c]
T30	174.7 ± 0.7[d]	217.5 ± 3.2[c]	276.9 ± 1.5[c]	39.0 ± 0.7[c]	217.8 ± 40.4[c]
T40	177.3 ± 1.0[ef]	216.9 ± 2.7[c]	274.3 ± 0.3[d]	41.3 ± 1.1[d]	154.6 ± 25.7[c]
T50	179.3 ± 1.2[f]	212.4 ± 0.9[cd]	273.4 ± 0.4[d]	40.0 ± 1.0[cd]	240.4 ± 8.0[c]
T60	176.2 ± 0.8[de]	210.4 ± 0.9[d]	269.1 ± 0.1[e]	40.0 ± 0.5[cd]	225.4 ± 7.0[c]

weight loss ($T_{1\%}$), maximum degradation temperatures of the first (T_{max1}) and second (T_{max2}) decomposition stages, and char residue content at 800 °C of the cross-linked chitosan films with different tannic acid loadings. There are three main thermal decomposition stages for the neat films. The initial thermal decomposition stage occurring below 100 °C, attributed to moisture evaporation, was not observed, as all samples were preconditioned at 110 °C to remove moisture.[59] The subsequent transition stage, attributed to the degradation of the deacetylated part within the chitosan structure, occurs at 130–220 °C.[60] Furthermore, the major thermal decomposition stage, resulting from the breakage of the glycosidic bonds between N-glucosamine and N-acetylglucosamine rings, occurs within the temperatue range of 220–400 °C.[9,10,61] The DTG curve of the uncross-linked chitosan films (T0) revealed two main decomposition steps, displaying the maximum decomposition temperatures of 187.6 °C (T_{max1}) and 285.1 °C (T_{max2}), with a $T_{1\%}$ of 157.1 °C. With tannic acid, the first major decomposition step shifted to a higher temperature of 202.2 °C, and the $T_{1\%}$ of the T10 films increased to 162.5 °C. Notably, with the increase in the tannic acid concentration, the thermal stabilities of the cross-linked chitosan films were significantly improved ($p < 0.05$). The T40 and T50 materials showed $T_{1\%}$ values of 177.3 °C and 179.3 °C, respectively. The considerable rise in the initial stage of the thermal stabilities (>250 °C) was attributed to the cross-linking of the functional groups in chitosan and tannic acid. Meanwhile, the second major decomposition peak exhibited decreased intensity and shifted to a lower temperature. The T_{max2} of T10 decreased from 285.1 °C to 282.6 °C. T_{max2} decreased continuously with increasing tannic acid content. T60 showed a T_{max2} of 269.1 °C.

The reduced intensity of the T_{max2} peak might be due to the lower chitosan content in films, while the peak shift could be attributed to the increased amorphous regions. This was consistent with the disappearance of the crystalline peaks in the XRD curves of the cross-linked films with higher tannic acid contents. The lower major thermal degradation temperature of tannic acid compared with chitosan could also contribute.[43,62]

Moreover, the introduction of tannic acid influenced the char residue content at 800 °C. T0 exhibited a char content of 34.8 ± 1.3% after heating to 800 °C, which significantly increased to 36.7 ± 1.1% with 10 wt% tannic acid.

Subsequently, a greater tannic acid loading resulted in a higher char residue content, reaching a maximum of 41.3 ± 1.1% for the T40 films. This increase in the char content strongly suggests the formation of cross-linking between chitosan and tannic acid, which aligns with XPS results. Similar observations of the increased char content were reported in studies involving cross-linked casein[3] and cross-linked chitosan films.[63] Although the introduction of tannic acid caused a decrease in maximum degradation temperature, a significant shift in early degradation temperature to a higher temperature (an increase in $T_{1\%}$) was observed for the cross-linked chitosan films.

3.4 Gel content and water uptake

The gel content is a method used to provide a relative measure of cross-linking.[64,65] Fig. 4(c) shows the gel contents of the cross-linked chitosan films with tannic acid. The neat chitosan films showed a gel content of 44.4 ± 2.2%, ascribed to the strong interfacial interactions between chitosan functional groups. With introduction of tannic acid, the T10 films presented a significantly higher gel content of 54.7 ± 5.7% compared with the uncross-linked chitosan films (T0). This indicated the generation of cross-linking. However, increasing the tannic acid content led to a significant reduction in gel content. The gel content of the T60 films dropped to 14.0 ± 7.6%. This considerable reduction may be attributed to the reduced chitosan content in the films and the solubility of excessive unreacted tannic acid.[27] Additionally, this decline could be due to the predominance of hydrogen bonding over covalent bonding in the chitosan-tannic acid films.[27,66] Unlike covalent bonds, hydrogen bonds are more susceptible to disruption by water molecules, which may further contribute to the reduced gel content.[67]

Water sensitivity limits the use of bio-based films in packaging applications.[3] We investigated the water uptake capacity of the chitosan films incorporated with tannic acid. Fig. 4(d) shows the water uptake behaviors of the chitosan films with different tannic acid loadings over immersion times, while Table 2 presents their water absorption values at 72 h immersion time. The neat chitosan films absorbed water at a rate exceeding 10 times their weight within the first 60 min of immersion. The rapid water uptake was facilitated by the presence of amino and hydroxyl groups within the chitosan

structure, along with the hydroxyl or aldehyde groups at the chitosan chain ends, enhancing interaction with water molecules.[17,18] Subsequently, the water absorption by chitosan films continued at a slower rate with increased immersion time. After 48 h, the water absorption reached a saturation point, stabilizing at ~24 times their weight.[68] For the chitosan films with tannic acid, similar water absorption behavior was observed. These cross-linked films exhibited initial rapid water absorption within the first 60 min, followed by a slower water absorption rate until saturation. Comparable water absorption trends were observed for biomaterials and biocomposites.[68] For example, Kamaludin *et al.*[68] observed that higher chitosan contents facilitated greater water molecule diffusion in the composites due to chitosan dissolution.

Furthermore, with incorporating tannic acid, a significant reduction in water uptake ($p < 0.05$) was observed. The T10 films showed a water uptake value of $725.4 \pm 95.2\%$ at 72 h of immersion, respectively. This considerable reduction would be attributed to the cross-linking between tannic acid and functional groups of chitosan molecules, leading to their fewer available functional groups to interact with water molecules. As the tannic acid content increased, the water uptake of the cross-linked chitosan films decreased. The T20 materials absorbed $315.7 \pm 34.8\%$ of water after 72 h of immersion. However, at greater than 20 wt% tannic acid content, no significant change in water uptake was observed. This could be due to the decreased availability of chitosan molecules for interaction with water and the potential release of tannic acid. A similarly nonsignificant influence of tannic acid on moisture content was reported in casein films with >8 wt% tannic acid.[3] Importantly, the cross-linked chitosan films reached the equilibrium stage of water absorption in a shorter immersion time than the neat chitosan films due to the limited functional groups in the cross-linked chitosan films.

3.5 Wettability

The hydrophobicity or hydrophilicity of a material can be evaluated using water contact angle measurements. A contact angle greater than 90° indicates hydrophobic behavior, while a contact less than 90° suggests hydrophilic behavior.[69,70] For packaging films intended for food with high moisture content, a high water contact angle is desirable.[70] Fig. 5 presents the water contact angles of the cross-linked chitosan films containing various tannic acid concentrations. All cross-linked chitosan films exhibited water contact angles greater than 90°, indicating their hydrophobic nature. This hydrophobicity was attributed to the orientation of chitosan's functional groups, such as hydroxyl and amino groups, parallel to the film surfaces during drying process.[71,72]

The T0 film exhibited a water contact angle of $105.6 \pm 1.7°$, which was higher than the value previously reported for chitosan films.[70] This difference could be due to various factors such as the molecular weight of chitosan, its degree of acetylation, and processing conditions. Moreover, the water contact angle of chitosan was reported to decrease over time due to water adsorption and swelling of chitosan.[7,70] With the incorporation of tannic acid, the water contact angle of the cross-linked chitosan film significantly decreased ($p < 0.05$). This reduction could be attributed to the presence of tannic acid, which contains multiple phenolic hydroxyl groups in its structure, increasing the hydrophilicity of the chitosan film surface.[73] A similar trend was reported for chitosan films incorporated with green tea polyphenols, where the contact angle dropped from 84.6° to 36.5°.[74]

Additionally, the concentration of tannic acid used may influence the surface polarity. The addition of a small amount of citric acid (3 wt%) to starch films increased the water contact angle from 26.9° to 35.9°. However, when the citric acid content exceeded 3 wt%, the water contact angle decreased considerably. This reduction might be owing to the presence of unreacted citric acid, which contains one hydroxyl group and three carboxylic groups, increasing the hydrophilicity of the film surface.[75] A similar trend was observed in chitosan/gelatin membranes cross-linked with potassium pyroantimonate (PA). The water contact angle of the membranes considerably increased with PA content up to 5%, but further increases in PA loading beyond this threshold led to a decrease in the contact angle.[76]

3.6 Mechanical properties

The mechanical properties of food packaging materials are crucial for safeguarding food produce during transport and storage. Fig. 6 presents the tensile stress, Young's modulus, and elongation at break of the chitosan films at different tannic acid concentrations. The neat chitosan films without tannic acid (T0) showed tensile stress, Young's modulus, and elongation at break of 62.5 ± 8.4 MPa, 1.8 ± 0.4 GPa, and $60.5 \pm 7.6\%$, respectively. The introduction of tannic acid significantly enhanced the mechanical properties of the chitosan films ($p > 0.05$). For instance, tensile stress and Young's modulus of the T20 materials considerably increased to 83.3 ± 7.6 MPa and 3.0 ± 0.5 GPa, respectively. This improvement was attributed to the increased formation of cross-linking.[3,58] With increasing tannic acid concentration, the mechanical properties of the cross-linked chitosan films continued to improve. The tensile stress
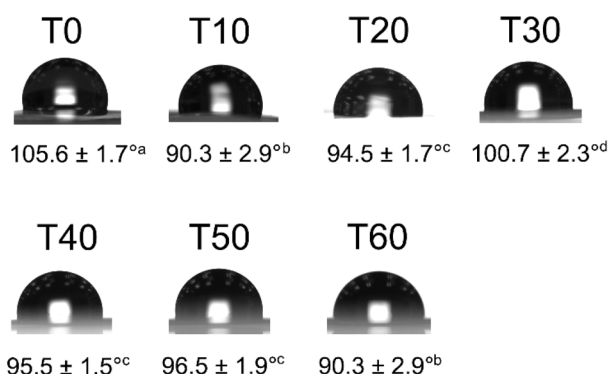

Fig. 5 Water droplets on the cross-linked chitosan film surfaces. Superscript letters represent significant differences ($p < 0.05$) among the samples tested under the same conditions.
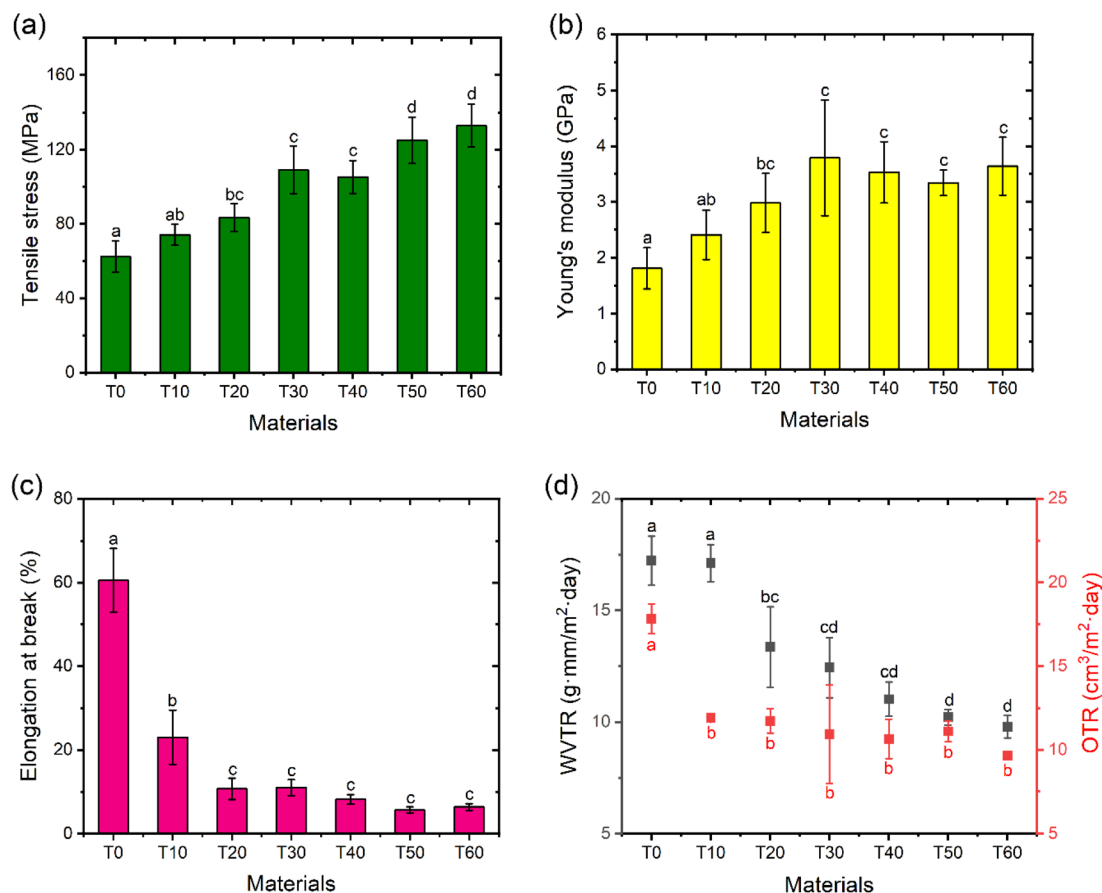
T0 — $105.6 \pm 1.7°^a$
T10 — $90.3 \pm 2.9°^b$
T20 — $94.5 \pm 1.7°^c$
T30 — $100.7 \pm 2.3°^d$
T40 — $95.5 \pm 1.5°^c$
T50 — $96.5 \pm 1.9°^c$
T60 — $90.3 \pm 2.9°^b$

Fig. 6 Mechanical and barrier properties of the cross-linked chitosan films with different tannic acid loadings: (a) tensile stress, (b) Young's modulus, (c) elongation at break, and (d) water vapor transmission rate (WVTR) and oxygen transmission rate (OTR). Superscript letters represent significant differences ($p < 0.05$) among the samples tested under the same conditions.

and Young's modulus of the T50 films increased to 125.0 ± 12.5 MPa and 3.3 ± 0.2 GPa, respectively, demonstrating 99.9% and 84.5% improvement, compared with the neat chitosan films. However, it is worth noting that beyond 50 wt% tannic acid loading, the tensile stress and modulus of the cross-linked films did not exhibit continuous improvement. Similarly, the introduction of tannic acid in poly(vinyl alcohol) hydrogels was reported to enhance their mechanical properties.[21] Furthermore, we observed the degradation in the flexibility of the chitosan films with tannic acid, causing them to be brittle. The elongation at break of T10 drastically decreased from 60.5 ± 7.6% to 23.1 ± 6.5%. The brittleness became more pronounced with higher tannic acid loading. The elongation at break of T60 significantly decreased ($p < 0.05$) by 89.5% to 6.4 ± 0.8%.

The mechanical properties of the cross-linked chitosan films with tannic acid, prepared in this work, were compared to those of petroleum-based and bio-based packaging films, as summarized in Table 3. These cross-linked chitosan films demonstrated superior tensile stress and Young's modulus to commercial petroleum-based food packaging films: low-density polyethylene (LDPE) (tensile stress: 19 ± 1 MPa and modulus: 0.21 ± 0.01 GPa),[77] high-density polyethylene (HDPE) (tensile stress: 38 ± 4 MPa and modulus: 1.07 ± 0.08 GPa),[77] and polypropylene (PP) (tensile stress: 28.7 ± 2.2 MPa and modulus: 2.0

± 0.2 GPa).[78] The mechanical properties of these cross-linked films closely approached those of poly(ethylene terephthalate) (PET) (tensile stress: 100 MPa and modulus: 4.8 GPa).[79] However, the elongation at break of the cross-linked chitosan films was comparable to PP (17.8 ± 9.7%) and higher than PET (2.5%) but significantly lower than HDPE (615 ± 47%) and LDPE (182 ± 30%). Also, when compared with poly(lactic acid) (PLA) and other natural polymers such as gelatin and starch, the cross-linked chitosan films exhibited greater mechanical properties. This suggests the potential of the developed cross-linked chitosan films to replace both petroleum-based and bio-based packaging materials. However, it is essential to acknowledge that these films have limitations in high-flexibility applications. This limitation was attributed to the cross-linking and hydrogen bonding which hinders the movement of molecular chains of chitosan.[28] Therefore, our forthcoming efforts will be focused on developing bio-based films with improved flexibility while maintaining their mechanical properties.

3.7 Barrier properties

Barrier properties are important for packaging applications; thus, we explored the effects of tannic acid on the barrier properties of the chitosan films. Fig. 6(d) presents the WVTR and OTR

Table 3 Mechanical properties of commercial petroleum-based and bio-based packaging films. Superscript letters represent significant differences ($p < 0.05$) among the chitosan samples prepared in this work tested under the same conditions

Material	Tensile stress (MPa)	Young's modulus (GPa)	Elongation at break (%)	Ref.
Commercial petroleum-based packaging films				
Low-density polyethylene (LDPE)	19 ± 1	0.21 ± 0.01	182 ± 30	77
High-density polyethylene (HDPE)	38 ± 4	1.07 ± 0.08	615 ± 47	77
Polypropylene (PP)	28.7 ± 2.2	2.0 ± 0.2	17.8 ± 9.7	78
Poly(ethylene terephthalate) (PET)	100	4.8	2.5	79
Bio-based packaging films				
Poly(lactic acid) (PLA)	61 ± 2	2.97 ± 0.05	4 ± 1	77
Thermoplastic starch	2.37 ± 0.23	0.05 ± 0.01	35.6 ± 5.5	4
Gelatin	9.6 ± 2.3	0.26 ± 0.01	23.4 ± 1.6	80
Chitosan (T0)	62.51 ± 8.42^{a}	1.81 ± 0.37^{a}	60.53 ± 7.64^{a}	This work
T10	74.18 ± 5.56^{ab}	2.41 ± 0.44^{ab}	23.05 ± 6.48^{b}	This work
T30	109.04 ± 12.86^{c}	3.79 ± 1.04^{c}	10.98 ± 1.91^{c}	This work
T50	124.96 ± 12.50^{d}	3.34 ± 0.23^{c}	5.61 ± 0.75^{c}	This work

of the chitosan films with different tannic acid concentrations. T0 exhibited a high WVTR value of 17.23 ± 1.10 g mm per m^2 per day due to its hydrophilicity. The incorporation of tannic acid resulted in a significant reduction in the WVTR of the chitosan films ($p < 0.05$). This reduction could be attributed to delayed water vapor transportation through films and a decrease in the available functional groups in chitosan to interact with water molecules. These changes resulted from cross-linking. The WVTR values of the T20 and T30 films were 13.36 ± 1.79 and 12.44 ± 1.34 g mm per m^2 per day, respectively. A similar decrease in WVTR was observed when nanocellulose-coated paper used citric acid as a cross-linker.[81] Shahriari et al.[82] also reported a reduction in WVTR and OTR of biaxial-oriented PP with a high cross-linked coating. However, greater than 30 wt% tannic acid concentration, no significant change in WVTR was observed. This might be due to a higher fraction of unreacted tannin acid in the film. Notably, the WVTR of the T30 films was considerably lower than those of polyamide 11 ($\sim$36 g mm per m^2 per day) and polyamide 12 ($\sim$25 g mm per m^2 per day)[83] but slightly higher than that of PLA ($\sim$6 g mm per m^2 per day).[84]

Moreover, the OTR of the chitosan films cross-linked with tannic acid was evaluated (Fig. 6(d)). T0 presented an OTR value of 17.81 ± 0.89 cm^3 per m^2 per day. With the introduction of tannic acid, a considerable reduction in OTR was observed. This decrease was attributed to the strong interaction through the formation of a cross-linking network within the chitosan films, resulting in an increased diffusion pathway of oxygen.[85] However, as the tannic acid loading increased from 10 to 60 wt%, no significant change in the OTR of the chitosan films was noticed. All cross-linked chitosan films with tannic acid exhibited OTR values of $\sim$10 cm^3 per m^2 per day, which is considerably lower than those of petroleum-based PET (34.71 cm^3 per m^2 per day), PP (3642 cm^3 per m^2 per day), and HDPE (2783 cm^3 per m^2 per day) and biodegradable polymers and biopolymers such as PLA (410 cm^3 per m^2 per day),[86] poly(-butylene adipate-co-terephthalate) (1530 cm^3 per m^2 per day),[86] cellulose acetate (650 cm^3 per m^2 per day),[86] and pea-based thermoplastic starch (276 cm^3 per m^2 per day).[86] The comparison of the WVTR and OTR results of the developed cross-linked

chitosan films with those of petroleum-based polymers and biopolymers indicates that the cross-linked chitosan films exhibit promising barrier properties, positioning them as potential candidates for packaging applications.

3.8 Morphology

Fig. 7 presents the fracture surfaces of the cross-linked chitosan films with various tannic acid concentrations after tensile
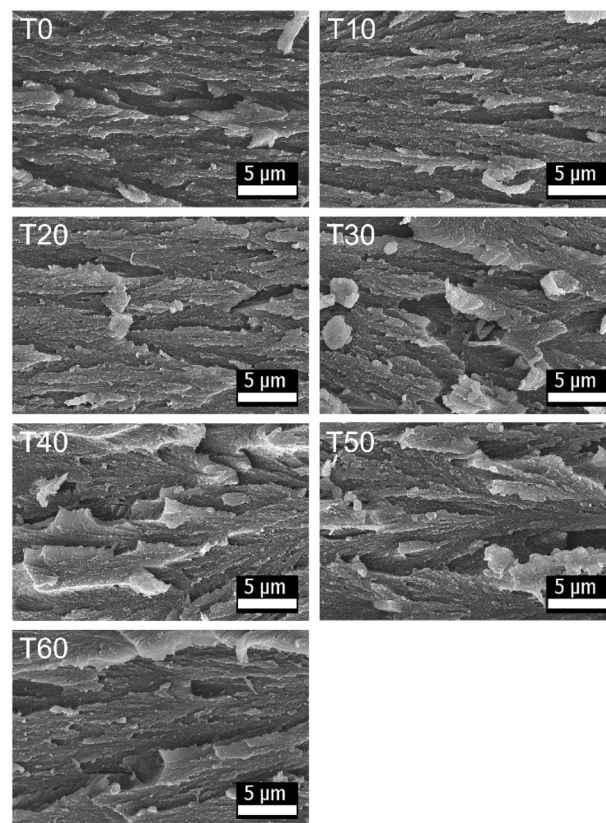

Fig. 7 Fracture surfaces of the cross-linked chitosan films with different tannic acid loadings.

deformation. The morphology of the neat chitosan films (T0) changed noticeably after the addition of tannic acid. The T0 film exhibited an elongated structure formed during tensile deformation, indicating a higher elongation at break (60.5 ± 7.6%). A similar architecture was observed for the T10 film, which corresponded to a high elongation at break of 23.1 ± 6.5%. However, as the tannic acid concentration increased beyond 10 wt%, the fracture surface morphology of the cross-linked chitosan composite films became noticeably rougher. This roughness was attributed to the formation of cross-linking, which hinders the stretching and elongation of chitosan molecular chains and restricts bond angle rotation.[28]

3.9 Antibacterial properties

The antimicrobial properties of the cross-linked chitosan films were qualitatively evaluated through the agar diffusion assay, and the results are shown in Fig. 8. *E. coli* and *S. aureus* were used as Gram-negative and Gram-positive bacterial indicators, respectively. The chitosan film without tannic acid (T0) exhibited a clear zone of inhibition against both *E. coli* and *S. aureus*. Meanwhile, the film containing 10% tannic acid (T10) inhibited only *S. aureus*. Conversely, the films with higher tannic acid contents (T20, T30, T40, T50, and T60) were ineffective against all tested bacteria (Fig. 8(b)). The proposed antimicrobial mechanism of chitosan is based on electrostatic interactions. A previous study[87] suggested that the antimicrobial activity of the chitosan is correlated with the number of cationized groups. The narrow antimicrobial spectra observed in the cross-linked chitosan films here may be attributed to the lack of uncross-linked chitosan molecules with cationized groups. The higher tannic acid content in the films resulted in the higher degree of chitosan cross-linking, leading to the reduced availability of active cationized chitosan molecules for interaction with

bacterial cells. Tanpichai *et al.*[88] demonstrated that chitosan only inhibited the growth of *E. coli* and *S. aureus* when tested in its solution (uncross-linking) form. However, when the same active chitosan was coated on another material such as cellulose paper, no clear zone of bacterial inhibition was observed. A similar adverse effect of the cross-linker on the antimicrobial efficiency of the chitosan film was also observed by Liang *et al.*[89] In contrast to the findings reported by Lee *et al.*,[27] the antimicrobial efficiency of the chitosan films with tannic acid investigated here demonstrated a different result. Chitosan films with a higher tannic acid loading exhibited greater antibacterial activity against both *E. coli* and *S. aureus*. The enhanced antibacterial activity observed might potentially be attributed to the release of tannic acid weakly bound with chitosan. Notably, the molecular weight of chitosan used here (2100 kDa) differs from that used in the work of Lee *et al.* (295 kDa), which could influence interactions between chitosan and tannic acid. Exploring the effects of the molecular weight of chitosan interacting with tannic acid on the properties of their films would be the focus of our future research work. We also observed that *S. aureus* displayed greater sensitivity to the chitosan films than *E. coli*. This differential sensitivity may be attributed to variations in bacterial surface structures that affect the efficacy of chitosan. Generally, the outer cell surface of Gram-positive bacteria is mainly composed of a thick peptidoglycan layer, with numerous pores that facilitate the attachment and/or entry of foreign molecules into the cell. Meanwhile, the outer surface of Gram-negative bacteria is shielded by a lipid and phospholipid layer, acting as a potential barrier against foreign molecules, especially those with high-molecular-weight compounds (*i.e.*, chitosan). Therefore, it is not surprising that the cross-linked chitosan films exhibited a greater likelihood of activity against Gram-positive *S. aureus* compared with Gram-negative *E. coli*.

Although increasing the tannic acid concentration improved the mechanical and barrier properties of the cross-linked chitosan-based films, it led to a deterioration in the antibacterial properties of the films. The loss of the antibacterial functionality could limit the films' suitability for packaging applications. To address this limitation, future work will focus on incorporating chitin nanofibers, which possess a similar structure to chitosan, into the cross-linked chitosan films to enhance the antibacterial performance.[10] Additionally, the addition of antibacterial nanoparticles, such as titanium dioxide or silver nanoparticles, will be explored to further improve the antimicrobial properties of the cross-linked chitosan films.[90–92]

3.10 Packaging application for extending the shelf life of chilies

The T30 films were selected to develop biodegradable packaging intended for extending the shelf life of fresh food produce, as shown in Fig. 9(a), due to their promising characteristics, including transparency, UV-blocking capability, mechanical performance, and barrier properties. The T30 packaging, as shown in Fig. 9(b), demonstrates high light transparency,
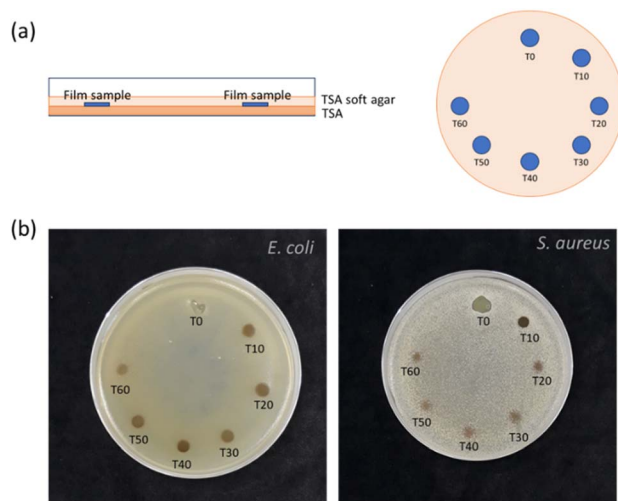

Fig. 8 Antibacterial properties of the cross-linked chitosan films with different tannic acid concentrations: (a) schematic diagram of the agar diffusion antimicrobial activity assay and designated positions for the cross-linked chitosan films with tannic acid and (b) antimicrobial activity of the cross-linked chitosan film samples.
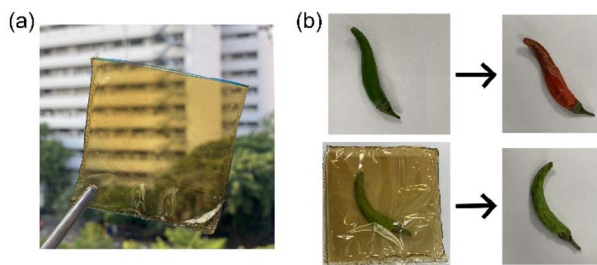
Fig. 9 Packaging for extending the shelf life of chilies: (a) packaging developed from the T30 films and (b) visual appearance of chilies, both unpacked (upper panel) and packaged (lower panel), on days 0 and 7 of storage.

allowing visibility of the packaged chili. However, its yellowness might hinder consumer appeal by altering the original color of the product. Therefore, this packaging may be better suited for products where visual appearance is not a critical factor. Also, increasing public awareness of the environmental benefits of bio-based packaging can boost consumer interest in sustainability and enhance acceptance of visual limitations such as minor discoloration. Packaging plays a crucial role in shaping consumer perceptions and attitudes towards food products.[93–95] Recent studies have shown that environmental considerations significantly influence purchase decisions.[93,94] Consumers with strong environmental awareness are more likely to prefer products packaged in eco-friendly materials.

The effectiveness of this packaging was assessed by preserving chilies. Fig. 9(b) compares the unpacked chilies, as control, and those packaged in T30 packaging, stored at room temperature for 7 days. Initially (day 0), all chilies were uniformly green with a smooth and glossy surface. On day 7 of storage, the color of the unpacked chilies completely changed from green to red and surface shrinkage and dryness were observed. Meanwhile, those stored in the T30 packaging retained their green hue and displayed fewer wrinkles on the surface. This preservation of their green color and reduced wrinkling could be due to the minimized moisture evaporation from the chilies stored in the T30 packaging compared with unpacked chilies.[96] Moreover, the T30 packaging can prevent UV transmission, reducing the oxidation and deterioration of the chilies. The natural ripening process of green chilies, caused by metabolic processes and respiration, is clearly observed through their color transition from green to red.[97–99] This transformation occurs due to two mechanisms: chlorophyll degradation and carotenoid accumulation. As chilies ripen, carotenoid concentration increases, intensifying the red coloration.[99] Therefore, the prepared cross-linked chitosan films with tannic acid show promise in prolonging the shelf life of chilies and preserving their quality. Our future research work will explore broader application studies of these films to extend the shelf life of different fresh produce with a focus on their physiological characteristics such as color parameters, firmness, and weight loss.

Moreover, the degradation behavior of chitosan films is a critical consideration for their practical applications. As a bio-based polymer, chitosan films showed fragmentation and partial degradation at the edges after just 3 days of soil burial.[74] In the study by Feky *et al.*,[100] over 40 wt% of the original weight of chitosan films decomposed within 7 days under soil-burial conditions, whereas PP packaging films remained unaffected. Complete degradation of chitosan films was reported after 24 weeks in soil.[101] This biodegradation is driven by a combination of biodeterioration, fragmentation, mineralization, and metabolism, converting the material into carbon dioxide, methane, water, biomass, and humic matter.[101] The degradation rate of chitosan films depends on several factors such as soil characteristics, microbial activity, physiochemical characteristics of the materials, and environmental conditions.[74,100,101] Moreover, Westlake *et al.*[101] investigated the degradation of chitosan films cross-linked with gallic acid in deionized water and seawater. After 12 weeks, the cross-linked films exhibited a noticeable weight reduction, 32.6% in water and 43.1% in seawater. This mass loss was mainly attributed to fragmentation.[101] It should be noted that the slower degradation observed in aqueous environments, compared to soil, might be due to a lower concentration of bacteria and microorganisms.[70] Although chitosan films are compostable under environmental conditions, their direct application in high-moisture or water-contact scenarios may be limited. Based on the water uptake and gel content analyses of the cross-linked chitosan-based films developed in this work, prolonged exposure to moisture and water might result in fragmentation or leaching of chitosan into aqueous environments. Therefore, improving the water resistance of these films will be a primary objective in our future work, with the goal of developing sustainable packaging alternatives to petroleum-based films.

Additionally, it has been reported that residual acetic acid remained within chitosan films after drying. ~0.5% of acetic acid was measured in the dried films prepared from a 1% chitosan solution dissolved in 1% acetic acid.[102] The amount of acetic acid measured from the dried chitosan was lower than the initial acetic acid concentration, likely due to volatilization during the drying process. The residual acetic acid in the chitosan films can act as a plasticizer, causing a looser film structure that compromises both mechanical properties and water vapor barrier properties. To address this issue, the use of alternative solvents such as citric acid or tannic acid for dissolving chitosan or the incorporation of a neutralization step to remove residual acetic acid from the films would be considered.

4 Conclusion

We successfully incorporated tannic acid into chitosan. The influence of tannic acid loadings on the properties of the cross-linked chitosan films was evaluated. The introduction of tannic acid into chitosan effectively blocked both UV-B and UV-A rays. The UV-blocking efficiencies of the films increased with an increasing tannic acid loading, reaching an optimal level at 30 wt%, while maintaining a transparency of greater than 85%. Moreover, the formation of cross-linking *via* Schiff-base covalent bonding and hydrogen bonding between chitosan and tannic improved the thermal stability, water uptake, gel content, mechanical performance, and barrier properties of the films, but

decreased the water contact angle. Specifically, the water uptake of the chitosan films with 30 wt% tannic acid significantly reduced by ∼90% to 217.8% compared with the neat chitosan films (2415.5%). However, when the tannic acid concentration exceeded 30 wt%, its effects on water uptake, mechanical properties, and water vapor permeability of the films were slightly diminished, possibly due to a decreased availability of chitosan molecules for interaction with water. Furthermore, the antibacterial properties of the neat chitosan films against *E. coli* and *S. aureus* diminished with the incorporation of tannic acid. Moreover, the prepared chitosan films with tannic acid were used to develop the packaging, which effectively prolonged the shelf life of chilies and preserved their quality. Compared with petroleum-based polymers and biopolymer packaging films, the prepared cross-linked chitosan films with tannic acid demonstrated superior mechanical and barrier properties as well as great UV-shielding capability and transparency to extend the shelf life of food produce and protect them from sunlight. Therefore, these films hold significant potential as alternatives to petroleum-based polymer materials for packaging applications.

Author contributions

Supachok Tanpichai: conceptualization; data curation; formal analysis; funding; investigation; methodology; project administration; resources; writing – original draft; writing – review & editing. Kitti Yuwawech: data curation; formal analysis; methodology. Ekachai Wimolmala: data curation; formal analysis. Yanee Srimarut: data curation; formal analysis; methodology. Weerapong Woraprayote: data curation; formal analysis; investigation; methodology; roles/writing – original draft; writing – review & editing. Yuwares Malila: conceptualization; data curation; investigation; roles/writing – original draft; writing – review & editing.

Conflicts of interest

There are no conflicts to declare.

Data availability

All the data for the manuscript is available in the manuscript.

Acknowledgements

References

1 R. Geyer, J. R. Jambeck and K. L. Law, *Sci. Adv.*, 2017, **3**, e1700782.

2 L. Lebreton, M. Egger and B. Slat, *Sci. Rep.*, 2019, **9**, 12922.

3 M. L. Picchio, Y. G. Linck, G. A. Monti, L. M. Gugliotta, R. J. Minari and C. I. Alvarez Igarzabal, *Food Hydrocoll.*, 2018, **84**, 424–434.

4 S. Tanpichai, K. Thongdonson and A. Boonmahitthisud, *J. Mater. Res. Technol.*, 2023, **26**, 5617–5625.

5 P. M. Coelho, B. Corona, R. ten Klooster and E. Worrell, *Resour. Conserv. Recycl.: X*, 2020, **6**, 100037.

6 M. A. Mahmud, S. A. Belal and M. A. Gafur, *J. Mater. Res. Technol.*, 2023, **24**, 1856–1874.

7 A. Boonmahitthisud, C. Booranapunpong, C. Pattaradechakul and S. Tanpichai, *Int. J. Biol. Macromol.*, 2023, **240**, 124412.

8 S. Tanpichai, *eXPRESS Polym. Lett.*, 2022, **16**, 52–74.

9 A. Boonmahitthisud, K. Thongdonson and S. Tanpichai, *J. Nat. Fibers*, 2023, **20**, 2229515.

10 S. Tanpichai, L. Pumpuang, Y. Srimarut, W. Woraprayote and Y. Malila, *Sci. Rep.*, 2023, **13**, 13195.

11 T. Mehdizadeh, H. Tajik, S. M. Razavi Rohani and A. R. Oromiehie, *Vet. Res. Forum*, 2012, **3**, 167–173.

12 J. Liu, S. Liu, Y. Chen, L. Zhang, J. Kan and C. Jin, *Food Hydrocolloids*, 2017, **71**, 176–186.

13 M. Arkoun, F. Daigle, R. A. Holley, M. C. Heuzey and A. Ajji, *Packag. Technol. Sci.*, 2018, **31**, 185–195.

14 R. Priyadarshi and J. W. Rhim, *Innovative Food Sci. Emerging Technol.*, 2020, **62**, 102346.

15 A. Boonmahitthisud, T. Wongjampee and S. Tanpichai, *Carbohydr. Polym.*, 2025, **356**, 123373.

16 M. E. Domínguez-Espinosa, A. Fuentes-Ruíz, A. Arreola-González, T. d. J. Jaime-Ornelas, M. A. Morales-Ovando, J. M. E. Hernández-Méndez, M. d. C. Hernández-Cruz, R. I. Cruz-Rodríguez, T. Romero-Cortés, J. M. Tirado-Gallegos and A. Cruz-Salomón, *J. Food Process. Preserv.*, 2022, **46**, e16154.

17 S. Tanpichai, Y. Srimarut, W. Woraprayote and Y. Malila, *Int. J. Biol. Macromol.*, 2022, **213**, 534–545.

18 H. Gocho, H. Shimizu, A. Tanioka, T. J. Chou and T. Nakajima, *Carbohydr. Polym.*, 2000, **41**, 87–90.

19 Z.-Y. Zhang, Y. Sun, Y.-D. Zheng, W. He, Y.-Y. Yang, Y.-J. Xie, Z.-X. Feng and K. Qiao, *Mater. Sci. Eng., C*, 2020, **106**, 110249.

20 R. Tan, F. Li, Y. Zhang, Z. Yuan, X. Feng, W. Zhang, T. Liang, J. Cao, C. F. De Hoop, X. Peng and X. Huang, *J. Nanomater.*, 2021, **2021**, 4821717.

21 H. Fan, J. Wang and Z. Jin, *Macromolecules*, 2018, **51**, 1696–1705.

22 Y. Yuan, Q. Xue, Q. Guo, G. Wang, S. Yan, Y. Wu, L. Li, X. Zhang and B. Li, *Food Packag. Shelf Life*, 2021, **30**, 100747.

23 W. Liu, S. Kang, Q. Zhang, S. Chen, Q. Yang and B. Yan, *Food Chem.*, 2023, **410**, 135405.

24 A.-S. Glaive, T. Modjinou, D.-L. Versace, S. Abbad-Andaloussi, P. Dubot, V. Langlois and E. Renard, *ACS Sustain. Chem. Eng.*, 2017, **5**, 2320–2329.

25 Y.-N. Chen, L. Peng, T. Liu, Y. Wang, S. Shi and H. Wang, *ACS Appl. Mater. Interfaces*, 2016, **8**, 27199–27206.

26 B. Kaczmarek, A. Owczarek, K. Nadolna and A. Sionkowska, *Mater. Lett.*, 2019, **245**, 22–24.

27 S. J. Lee, M. A. Gwak, K. Chathuranga, J. S. Lee, J. Koo and W. H. Park, *Food Hydrocolloids*, 2023, **136**, 108249.

28 Z. Qin, Y. Huang, S. Xiao, H. Zhang, Y. Lu and K. Xu, *Int. J. Mol. Sci.*, 2022, **23**, 9284.

29 V. Acharya, A. Ghosh, A. R. Chowdhury and P. Datta, *Soft Mater.*, 2022, **20**, 149–160.

30 N. N. Bailore, B. K. Sarojini and K. R. Harshitha, *ACS Omega*, 2022, **7**, 27876–27885.

31 T. Chu, J. Shi, Y. Xia, H. Wang, G. Fan and M. Yang, *Ind. Crops Prod.*, 2022, **187**, 115327.

32 Y. He, H.-C. Ye, T.-T. You and F. Xu, *Food Hydrocoll.*, 2023, **137**, 108355.

33 T. Wu, Y. Xu, Z. Cui, H. Li, K. Wang, L. Kang, Y. Cai, J. Li and D. Tian, *ACS Sustain. Chem. Eng.*, 2022, **10**, 15380–15388.

34 S. Tanpichai and K. Oksman, *Composites, Part A*, 2016, **88**, 226–233.

35 H. Wu, Y. Lei, J. Lu, R. Zhu, D. Xiao, C. Jiao, R. Xia, Z. Zhang, G. Shen, Y. Liu, S. Li and M. Li, *Food Hydrocolloids*, 2019, **97**, 105208.

36 P. Ezati, A. Khan, R. Priyadarshi, T. Bhattacharya, S. K. Tammina and J.-W. Rhim, *Food Hydrocolloids*, 2023, **142**, 108771.

37 A. Costanzo, F. Fausti, G. Spallone, A. Narcisi and E. Botti, *Int. J. Dev. Biol.*, 2015, **59**, 73–78.

38 W. J. Grigsby, J. H. Bridson, C. Lomas and J.-A. Elliot, *Polymers*, 2013, **5**, 344–360.

39 M. T. Haqiqi, W. Bankeeree, P. Lotrakul, P. Pattanuwat, H. Punnapayak, R. Ramadhan, T. Kobayashi, R. Amirta and S. Prasongsuk, *ACS Omega*, 2021, **6**, 9653–9666.

40 H. Dai, Y. Chen, H. Chen, Y. Fu, L. Ma, H. Wang, Y. Yu, H. Zhu and Y. Zhang, *Food Chem.*, 2023, **401**, 134154.

41 X. Ran, Y. Qu, Y. Wang, B. Cui, Y. Shen and Y. Li, *J. Compos. Sci.*, 2023, **7**, 410.

42 S. Cohen, H. Haham, M. Pellach and S. Margel, *ACS Appl. Mater. Interfaces*, 2017, **9**, 868–875.

43 Y. Jing, Y. Diao and X. Yu, *React. Funct. Polym.*, 2019, **135**, 16–22.

44 G. R. Mahdavinia, A. Mosallanezhad, M. Soleymani and M. Sabzi, *Int. J. Biol. Macromol.*, 2017, **97**, 209–217.

45 M. Gatto, D. Ochi, C. M. P. Yoshida and C. F. da Silva, *Carbohydr. Polym.*, 2019, **210**, 56–63.

46 H. Mao, C. Wei, Y. Gong, S. Wang and W. Ding, *Polymers*, 2019, **11**, 166.

47 L. d. S. Soares, R. B. Perim, E. S. de Alvarenga, L. d. M. Guimarães, A. V. N. d. C. Teixeira, J. S. d. R. Coimbra and E. B. de Oliveira, *Int. J. Biol. Macromol.*, 2019, **128**, 140–148.

48 X. Xu, C. Gao, X. Feng, L. Meng, Z. Wang, Y. Zhang and X. Tang, *Int. J. Biol. Macromol.*, 2025, **308**, 142751.

49 V. Pawariya, S. De and J. Dutta, *Carbohydr. Polym.*, 2024, **323**, 121395.

50 W. Li, Z. Li, T. Liu, G. Du, K. Ni, H. Yang, H. Su, S. Liu, C. Yin, X. Ran, W. Gao and L. Yang, *Constr. Build. Mater.*, 2023, **398**, 132556.

51 N. Yousefzadeh, D. Habibi, M. H. Meshkatalsadat and M. Mahmoudiani Gilan, *J. Chem. Res.*, 2023, **47**, 17475198231183348.

52 A. Dutta and S. K. Dolui, *Appl. Surf. Sci.*, 2011, **257**, 6889–6896.

53 M. Hossain, P. Roy, C. Zakaria and M. K.-E. Zahan, *Int. J. Chem. Stud.*, 2018, **6**, 19–31.

54 L. Fabbrizzi, *J. Org. Chem.*, 2020, **85**, 12212–12226.

55 S. M. Costa, D. P. Ferreira, P. Teixeira, L. F. Ballesteros, J. A. Teixeira and R. Fangueiro, *Int. J. Biol. Macromol.*, 2021, **177**, 241–251.

56 X. Zhang, J. Liu, H. Yong, Y. Qin, J. Liu and C. Jin, *Int. J. Biol. Macromol.*, 2020, **145**, 1129–1139.

57 C. Qiao, X. Ma, J. Zhang and J. Yao, *Food Chem.*, 2017, **235**, 45–50.

58 E. Yildiz, A. A. Emir, G. Sumnu and L. N. Kahyaoglu, *Food Biosci.*, 2022, **50**, 102121.

59 Y. Lai, W. Wang, J. Zhao, S. Tu, Y. Yin and L. Ye, *Food Packag. Shelf Life*, 2022, **33**, 100879.

60 A. T. Paulino, J. I. Simionato, J. C. Garcia and J. Nozaki, *Carbohydr. Polym.*, 2006, **64**, 98–103.

61 J. Zawadzki and H. Kaczmarek, *Carbohydr. Polym.*, 2010, **80**, 394–400.

62 Z. Xia, A. Singh, W. Kiratitanavit, R. Mosurkal, J. Kumar and R. Nagarajan, *Thermochim. Acta*, 2015, **605**, 77–85.

63 F. López-Saucedo, L. Buendía-González, H. Magaña, G. G. Flores-Rojas and E. Bucio, *Polymers*, 2023, **15**, 2724.

64 H. Peidayesh, Z. Ahmadi, H. A. Khonakdar, M. Abdouss and I. Chodák, *Polym. Adv. Technol.*, 2020, **31**, 1256–1269.

65 C. Menzel, E. Olsson, T. S. Plivelic, R. Andersson, C. Johansson, R. Kuktaite, L. Järnström and K. Koch, *Carbohydr. Polym.*, 2013, **96**, 270–276.

66 T. Yamada, Y. Mizuno, L. Tian, T. Kitaguchi and T. Fujie, *Macromol. Chem. Phys.*, 2025, **226**, 2400220.

67 M. Chen, T. Runge, L. Wang, R. Li, J. Feng, X.-L. Shu and Q.-S. Shi, *Carbohydr. Polym.*, 2018, **200**, 115–121.

68 N. H. I. Kamaludin, H. Ismail, A. Rusli and S. S. Ting, *Iran. Polym. J.*, 2021, **30**, 135–147.

69 M. Lokanathan, E. Wikramanayake and V. Bahadur, *Mater. Res. Express*, 2018, **6**(4), 046507.

70 J. R. Westlake, M. Laabei, Y. Jiang, W. C. Yew, D. L. Smith, A. D. Burrows and M. Xie, *ACS Food Sci. Technol.*, 2023, **3**, 1680–1693.

71 A. G. Cunha, S. C. M. Fernandes, C. S. R. Freire, A. J. D. Silvestre, C. P. Neto and A. Gandini, *Biomacromolecules*, 2008, **9**, 610–614.

72 M. A. Hubbe, *Bioresources*, 2019, **14**(4), 7630–7631.

73 M. Hosseini, L. Moghaddam, L. Barner, S. Cometta, D. W. Hutmacher and F. Medeiros Savi, *Prog. Polym. Sci.*, 2025, **160**, 101908.

74 A. Oberlintner, M. Bajić, G. Kalčíková, B. Likozar and U. Novak, *Environ. Technol. Innovation*, 2021, **21**, 101318.

75 S. Yao, B.-J. Wang and Y.-M. Weng, *Food Packag. Shelf Life*, 2022, **32**, 100845.

76 J. Liu, S. Wang, K. Xu, Z. Fan, P. Wang, Z. Xu, X. Ren, S. Hu and Z. Gao, *Carbohydr. Polym.*, 2020, **236**, 115963.

77 C. Winotapun, S. Phattarateera, A. Aontee, N. Junsook, W. Daud, N. Kerddonfag and W. Chinsirikul, *Packag. Technol. Sci.*, 2019, **32**, 405–418.

78 C. Mhumak and C. Pechyen, *Walailak J. Sci. Technol.*, 2018, **15**, 765–777.

79 D. G. Howells, B. M. Henry, Y. Leterrier, J. A. E. Månson, J. Madocks and H. E. Assender, *Surf. Coat. Technol.*, 2008, **202**, 3529–3537.

80 S. Khedri, E. Sadeghi, M. Rouhi, Z. Delshadian, A. Mortazavian, J. Guimarães, M. fallah and R. Mohammadi, *LWT–Food Sci. Technol.*, 2021, **138**, 110649.

81 M. A. Herrera, A. P. Mathew and K. Oksman, *Cellulose*, 2017, **24**, 3969–3980.

82 L. Shahriari, M. Mohseni and H. Yahyaei, *Prog. Org. Coat.*, 2019, **134**, 66–77.

83 A. Kausar, *J. Plast. Film Sheeting*, 2020, **36**, 94–112.

84 A. Bhatia, R. K. Gupta, S. N. Bhattacharya and H. J. Choi, *J. Nanomater.*, 2012, **2012**, 249094.

85 L. Zhuang, X. Zhi, B. Du and S. Yuan, *ACS Omega*, 2020, **5**, 1086–1097.

86 B. Dalton, P. Bhagabati, J. De Micco, R. B. Padamati and K. O'Connor, *Catalysts*, 2022, **12**, 319.

87 N. A. Mohamed and M. M. Fahmy, *Int. J. Mol. Sci.*, 2012, **13**, 11194–11209.

88 S. Tanpichai, S. Witayakran, J. Wootthikanokkhan, Y. Srimarut, W. Woraprayote and Y. Malila, *Int. J. Biol. Macromol.*, 2020, **155**, 1510–1519.

89 J. Liang, R. Wang and R. Chen, *Polymers*, 2019, **11**, 491.

90 W. Zhang and J.-W. Rhim, *Food Packag. Shelf Life*, 2022, **31**, 100806.

91 J. Li, D. Zhang and C. Hou, *Bioengineering*, 2025, **12**, 19.

92 M. M. V. Rao, N. Mohammad, S. Banerjee and P. K. Khanna, *Hybrid Adv.*, 2024, **6**, 100230.

93 J. Macht, J. Klink-Lehmann and S. Venghaus, *Food Qual. Prefer.*, 2023, **109**, 104884.

94 A. Berthold, S. Guion and M. Siegrist, *Food and Humanity*, 2024, **2**, 100265.

95 K. Steiner and A. Florack, *Foods*, 2023, **12**, 3911.

96 K. Mondal, S. K. Bhattacharjee, C. Mudenur, T. Ghosh, V. V. Goud and V. Katiyar, *RSC Adv.*, 2022, **12**, 13295–13313.

97 R. Priyadarshi, Sauraj, B. Kumar and Y. S. Negi, *Carbohydr. Polym.*, 2018, **195**, 329–338.

98 T. Gasti, S. Dixit, R. B. Chougale and S. P. Masti, *Sustainable Food Technol.*, 2023, **1**, 390–403.

99 W. Pola, S. Sugaya and S. Photchanachai, *Antioxidants*, 2020, **9**, 203.

100 A. R. El Feky, M. Ismaiel, M. Yılmaz, F. M. Madkour, A. El Nemr and H. A. H. Ibrahim, *Sci. Rep.*, 2024, **14**, 11161.

101 J. R. Westlake, E. Chaloner, M. Laabei, F. Sgouridis, A. D. Burrows and M. Xie, *RSC Sustainability*, 2025, **3**, 2680–2695.

102 J. Xu, K. Liu, W. Chang, B.-S. Chiou, M. Chen and F. Liu, *Foods*, 2022, **11**, 1657.